Colloblasts act as a biomechanical sensor for suitable prey in *Pleurobrachia*

Townsend, JP[a, 1, *], **Merces, GOT**[b, c, *], **Castellanos, GP**[d], **and Pickering, M**[b, c]

[a]Department of Biochemistry and Biophysics, University of Pennsylvania, Philadelphia, Pennsylvania 19104
[b]School of Medicine, University College Dublin, Belfield, Dublin 4, Ireland, D04 V1W8
[c]UCD Centre for Biomedical Engineering, University College Dublin, Belfield, Dublin 4, Ireland, D04 V1W8
[d]Department of Biology, University of Puerto Rico at Cayey, Cayey, Puerto Rico 00736
[1]Corresponding author
[*]These authors contributed equally to this work

Summary statement

Ctenophore colloblast adhesive is found to be strong, but few colloblasts are simultaneously active, producing a weakly-adhering system. A physical model demonstrates how such a system may filter unsuitable prey.

Abstract

Ctenophores are a group of largely-planktonic, gelatinous carnivores whose most common method of prey capture is nearly a phylum-defining trait. Tentaculate ctenophores release an unknown proteinaceous adhesive from specialized colloblast cells lining their tentacles following prey contact with the tentacles. There exist no extant studies of the mechanical properties of colloblast adhesive. We use live microscopy techniques to visualize adhesion events between *Pleurobrachia pileus* colloblasts and probes of different surface chemistries in response to probing with varying contact areas. We further define two mechanisms of adhesion termination upon probe retraction. Adapting a technique for measuring surface tension, we examine the adhesive strength of tentacles in the ctenophore *Pleurobrachia bachei* under varying pH and bonding time conditions, and demonstrate the destructive exhaustion of colloblast adhesive release. We find that colloblast-mediated adhesion is rapid, and that the bonding process is robust against shifts in ambient pH. However, we find that the *Pleurobrachia* colloblast adhesive system is among the weakest biological adhesive systems yet described. We place this surprising observation into a broader ecophysiological context by modeling prey capture for prey of a range of sizes. We find that limited use of colloblast adhesive with high surface area contact is suitable both for capturing appropriately sized prey and rejecting, by detachment, prey above a certain size threshold. This allows *Pleurobrachia*, lacking a mechanism to directly "see" potential prey they are interacting with, to invest in capturing only prey of an appropriate size, decreasing the risk of injury.

ctenophore | colloblast | adhesion | prey | filter

Correspondence: ***jptownsendii@gmail.com***

Introduction

Ctenophores are a phylum of gelatinous zooplankton known for being voracious and efficient ambush predators (Bishop, 1968; Greene et al., 1986; Haddock, 2007; Tamm, 2014). Most species in the phylum fall within the class Tentaculata (Haddock, 2007), characterized by the presence of tentacles whose surface is covered with a type of cell unique to ctenophores—colloblasts (Franc, 1978; Haddock, 2007; Tamm, 2014; von Byern et al., 2010). The present study focuses on *Pleurobrachia bachei* and *Pleurobrachia pileus*, two closely related and morphologically similar ctenophores of the order Cydippida found in the inshore waters of the Pacific and Atlantic oceans, respectively. Members of this order possess a pair of tentacles with numerous, evenly-spaced, smaller tentilla extending perpendicularly off the main tentacle body. While hunting, cydippid ctenophores tend to keep their tentacles and tentilla extended, waiting for prey to drift into the resulting dragnet (Haddock, 2007; Tamm, 2014). When prey make contact with the tentacles, the colloblasts release their adhesive and bond to the prey, tethered by "spiral filaments" to the tentacle body (Franc, 1978; von Byern et al., 2010). Colloblasts have a bouquet-shaped morphology with an apical enlargement protruding from the tentacle surface. On contact with prey, the colloblast adhesive is released from its storage place, likely a collection of internal vesicles, bonding the colloblast to the prey. This discharging action presumably destroys the colloblasts, so these one-time use cells may be continually replaced by differentiation from epithelial stem cells. (Alié et al., 2011; Franc, 1978; Hernandez-Nicaise, 1991)

Ctenophores' hunting technique is reminiscent of the ambush strategy of orb weaver spiders (Greene et al., 1986) and the release of an adhesive from colloblasts in response to prey-contact is superficially similar to the harpoon-like stinging cells in cnidarians, called nematocytes or cnidocytes (Holstein and Tardent, 1984; Kass-Simon and Scappaticci, Jr., 2002; Nüchter et al., 2006; Tamm, 2014). Cnidocytes and colloblasts do not share a common evolutionary origin (Babonis et al., 2018), and the use of adhesive-, rather than venom-loaded cells distinguishes them further. The attachment of colloblasts to an organ such as the tentacles as opposed to an external structure like a spider's web, in addition to the unique cellular physiology of the colloblast, have made them a quasi-phylum-defining trait for ctenophores (Dunn et al., 2015).

Despite the conspicuousness of colloblast-covered adhesive tentacles as a trait, many physical and biochemical questions about colloblasts remain open: What do adhesion and dead-

hesion events look like? How strong is colloblast adhesive? How quickly does it bond to a target? Is adhesion affected by ambient water conditions? Understanding the answers to these questions would aid our understanding of colloblast adhesive as a unique biomaterial and inform the potential limitations it puts on ctenophore predation.

In this study, we apply live microscopy techniques to visualize adhesion between probes and tentacles of *Pleurobrachia pileus*, assessing the fates of individual colloblasts engaging in adhesion. We assess the impact of contact area on adhesion, in addition to comparing probes of different surface chemistries. We adapt instrumentation for measuring surface tension to measure the adhesive force exerted by the colloblast adhesive system of *Pleurobrachia bachei*. Using our method, we can control what region of the tentacle is probed as well as the ambient water conditions that the tentacle and its colloblasts experience.

Our data demonstrate that ctenophore prey capture, mediated by colloblast adhesion, is a robust mechanism that acts quickly to ensnare prey under a variety of conditions. Understanding of the adhesion strength of the system, and of individual colloblasts, is gained. Furthermore, the burgeoning understanding of colloblasts is itself integral to our understanding of ctenophore ecology in a rapidly changing marine environment as well as the role of this early-diverging animal lineage in the larger story of animal cell type evolution (Ryan et al., 2013).

Methods

Sample collection

Pleurobrachia pileus were collected from the Irish Sea at Howth Harbor, Dublin, Ireland (53.393060, -6.066148) using plankton nets with an associated collection chamber, then transferred into Kreisel tanks established at University College Dublin, School of Medicine. Tanks (Courtney et al., 2020) were circulated with natural sea water (Seahorse Aquariums, Dublin, Ireland) maintained at 10-15 °C and fed a 20 ml aliquot of live *Artemia* sp. every 20 minutes using an automated feeding apparatus until use within 2 months.

Pleurobrachia bachei were collected by dip cupping at the docks at the University of Washington's Friday Harbor Labs in Friday Harbor, WA. (48.545234, -123.012020). Live animals were shipped overnight to the University of Pennsylvania for testing, where they were held at 4-10 °C in a filtered seawater (FSW) refugium containing macroalgae and live rock from Friday Harbor. Animals were used in experimental trials within a week of arrival.

Microscopic observation of tentacles during mechanical probing

Two types of silicone arenas were fabricated for physical probing of *Pleurobrachia pileus* tentacles: one composed of a soft silicone ridge substrate (Smooth-On, Ecoflex 00-10, shore-hardness = 00-10) and one composed of a rigid silicone ridge substrate (Smooth-On, Dragonskin 10 Medium, shore-hardness = 10A). The silicone arenas were placed onto clean, dry, charged microscope slides (Superfrost® Plus, Thermo Scientific), and pressed firmly to ensure adhesion to the glass. Anchoring slits were cut into the two corners of the arena. *P. pileus* were used for all imaging experiments. A single portion of severed *P. pileus* tentacle was transferred into the arena with ~300 μl of natural sea water. The tentacle was orientated within the arena using clean fine-tip forceps, and each end of the tentacle fragment was manipulated into an anchor slit to maintain tentacle position.

Probes were generated from 1.75mm diameter filaments of polylactic acid polymer (PLA; Yellow PLA filament, Prusa, FLM-PLA-175-YEL) by heating segments and pulling to create a tapered strand. The strand was then cut perpendicularly to the probe to generate a flat, circular tip. Lysine probes were generated by immersing PLA probes in 50 $mg \cdot ml^{-1}$ poly-D-lysine in PBS until the solution was fully evaporated to coat the probe tips in lysine. Copepod probes were generated by coating the tip of a PLA probe in a small amount of clear nail varnish. A single copepod carcass (*Calanoida* sp. Seahorse Aquariums, Dublin, Ireland) was pressed into the nail varnish, and left to dry. A clean probe was brought into contact with the tentacle fragment (velocity = 20 $mm \cdot min^{-1}$) under 20X magnification video microscopy using an open source microscopy system (Courtney et al., 2020). Contact/compression was maintained for 5 seconds, followed by probe retraction (velocity = 5 $mm \cdot min^{-1}$) (Fig. 1).

Probing videos were manually analyzed in ImageJ (Schindelin et al., 2012) to assess the area of contact between probe and tentacle, the total number of colloblast adhesion events, the number of colloblasts showing adhesive failure (colloblast head detaching from probe), the distance at which the individual colloblast deadhesion events occurred, and the number of colloblasts remaining adhered to the probe tip following full retraction of the probe (colloblast tail severing events). The number of colloblasts actively adhered to the probe in these trials was computed by the following linear model. For any area compressed under the probe ($A_{compression}$), there will be a certain number of colloblasts contacted. *Pleurobrachia* sp. colloblasts are densely packed on the surface of the tentacle and have a diameter of ~5 μm. The exterior face of these colloblasts are roughly spherical, so they present a surface area of 19.63 μm^2 when approximated as a circle. Due to the effect of circle packing, the packing density of colloblasts is less than 1. Modeling the positioning of colloblasts with a hexagonal packing arrangement based on microscopic images, the packing density is estimated to be 0.9, meaning an overall colloblast surface area accounting for packing density of 21.63 $\mu m^2 (SA_{colloblast})$. Thus, the number of colloblasts contacted ($C_{contact}$) in any probing event will be

Eq. 1: $C_{contact} = A_{compression}/SA_{colloblast}$

Of these colloblasts, only some fraction will become adhered. Thus an additional factor, the colloblast activity

fraction (CAF), is required. This represents the fraction of colloblasts activated in response to physical probing, and ranges strictly from 0 (0% of colloblasts contacted adhere) to 1 (100% of the colloblasts contacted adhere). A constant term, B, accounts for any additional factors, such as a minimum number of colloblasts activated in response to any contact ($B > 0$) or a depressive effect within tentacles preventing any colloblast adhesive release until a compression area threshold is passed ($B < 0$). The equation then to calculate the number of colloblasts adhered ($C_{adhered}$) is,

Eq. 2: $C_{adhered} = CAF \cdot C_{Contact} + B$

As $C_{contact}$ is a factor of $A_{compression}$ and $SA_{colloblast}$, we can rearrange Eq. 2 into the following linear model, where $m = CAF/SA_{colloblast}$

Eq. 3: $C_{adhered} = m \cdot A_{compression} + B$

Assessment of adhesive force and adhesive ability

Measurement of the adhesive force between a probe and a severed tentacle was assessed using *Pleurobrachia bachei*. In the assessment of adhesive force, tentacles were dissected and immediately laid on clean, untreated glass slides (Corning Inc.; Corning, NY). Excess water was blotted from the tentacles using a Kimwipe (Kimberly-Clark; Roswell, GA), and 200 μl of 0.22 μm vacuum-filtered seawater was added back to the tentacle to form a droplet around it (Fig. 1). This prepared slide was then positioned in a Kibron EZ-Piplus single channel surface tensiometer with a 0.5 mm diameter DyneProbe probe with hydrophilic surface chemistry attached (Kibron Inc.; Helsinki). The probe has a flat contact surface profile, forming a circle 0.196 mm^2 in area. The probe was lowered onto the tentacle at a rate of 0.0125 $mm \cdot s^{-1}$, and allowed to rest on the surface of the tentacle to "cure" for a range of time intervals before being raised up, again at 0.0125 $mm \cdot s^{-1}$. Our reported values for adhesive force ($F_{adhesion}$) represent the difference between the maximum force experienced by the probe as it was being lifted off the tentacle and the force on the probe as it contacted the tentacle (Fig. 1). Though we refer to these values as "forces," or "adhesive strength" for lexical ease they are more properly considered as an adhesive pressure—the adhesive force experienced across the surface area of the probe. Because the contact area of our probe is similar to that of a ctenophore's small prey (Bishop, 1968), we report our values as ecologically relevant forces. Unless otherwise noted, different, randomly selected spots on fresh tentacles were used for each trial, the probe rested on the tentacle for 60 seconds, and the probe was cleaned between trials by heating the tip of the probe until red hot, then wiping the probe down with an ethanol-soaked Kimwipe

In order to assess adhesive depletion/buildup on a probe tip, the adhesive force assay described above was repeated, but modified to probe the same spot on a tentacle multiple times, either cleaning the probe in between these trials (adhesive depletion) or not (adhesive buildup). Two different tentacles were used for these two series of repeated measurements.

Assessment of the impact of contact time on adhesive force was performed using the adhesive force assay as described above, but the time the probe was allowed to rest on the tentacle to "cure" before being pulled up was varied from between 5 and 600 seconds. The lower bound of 5 seconds represents the smallest reliable time period for the tensiometer to reverse the probe movement after stopping.

To assess the effect of ambient pH on adhesive force, the assay described above was repeated with artificial seawater (ASW) of varying pH. ASW was composed of Instant Ocean Sea Salt (Instant Ocean; Blacksburg, VA) mixed with deionized water to a specific gravity of 1.025. ASW was filtered to 0.22 μm and the pH adjusted to the test value using either concentrated HCl or 10 M NaOH as measured with an Accumet AP125 pH meter (Fisher Scientific; Pittsburgh, PA). After mounting the tentacle on the glass slide and blotting away excess seawater, 10 μl of pH adjusted ASW was added to the tentacle to both rinse it and avoid shocking the tentacle with a sudden shift in pH. Then, this water was also blotted away and 200 μl of the same solution of pH adjusted ASW was added to form a droplet around the tentacle. This prepared slide was then tested as above.

Results

Compressive Force as a factor in stimulating adhesive release

Direct contact between a PLA probe and severed tentacular surface was not sufficient to trigger colloblast adhesion, indicating a minimum compressive force requirement for adhesive release (Fig. 2A). Retraction of a probe following tentacular compression allowed for visualization of individual colloblast adhesion events (Fig 2B). Individual colloblast adhesion events were terminated in one of two ways: 1) adhesive failure (de-adhesion event) (Fig. 2B), or 2) colloblast tail severing (Fig. 2C). The total number of colloblast adhesion events, and the proportion of the two termination modalities, were assessed for probing events with a soft ridge substrate (Fig 3A). The compression area for each probing trial was also calculated to examine the impact of contact area on the number of adhesion events observed. For probing studies using a soft ridge substrate, the factor $m = 0.0000287345$, and the intercept $B = 6.88$ (Theil's incomplete method, n=32) indicates a potential linear relationship between compression area and colloblast adhesion events. However, correlation analysis revealed no significant correlation between contact area and colloblast adhesion events (Spearman r, P=0.1473, two-tailed), indicating no impact of compression area on the number of colloblasts adhering.

When repeating the experiment using Dragonskin silicone as a ridge substrate, a significant positive correlation was identified between contact area and colloblast adhesion events (Spearman r, P=0.0467, two-tailed) (Fig 3A). Calculations of the colloblast adhesion event-contact area relationship differed substantially, with a colloblast activity factor of

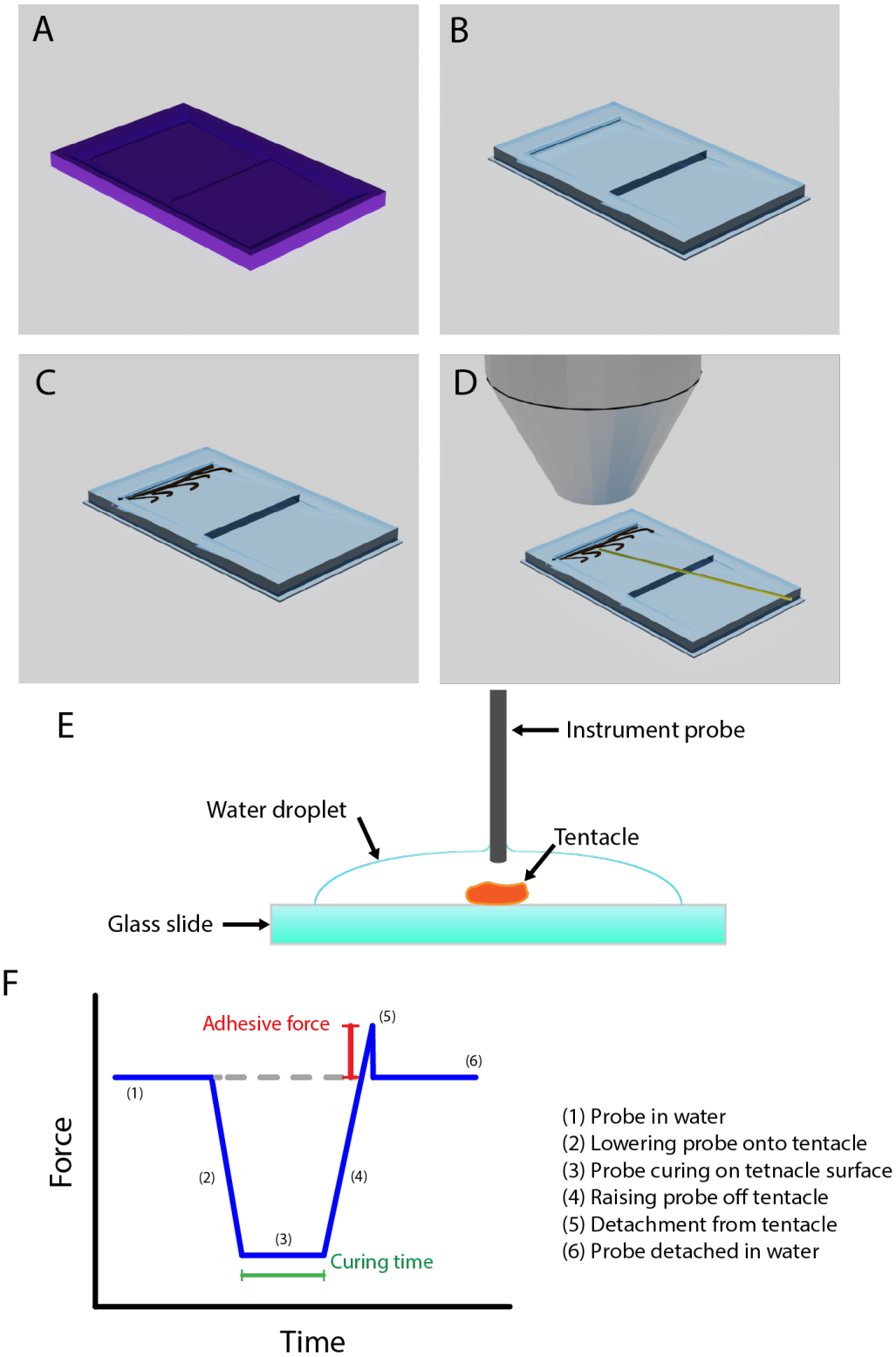

Figure 1. Experimental Methodology Design. Probing visualization: A) a 3D printed mould with two sloped regions was printed in PLA (0.15mm z-resolution, Prusa MK3). B) A negative of this mould was cast using either a firm silicone (Dragonskin shore hardness 10A) or soft silicone (Ecoflex, shore hardness 00-10), cured, and removed from the mould. C) A severed portion of tentacle from P. pileus was orientated within the ridge portion of a slope with ~300 μl of natural sea water. D) A probe of either PLA, lysine-coated PLA, or a copepod carcass was orientated using an XYZ micro-translator to be in proximity to the tentacle under 20X objective magnification. The micro-translator was mechanically coupled to the optics. For probing, the stage (which is decoupled from the optics/probe) was moved to bring the tentacle into contact with the probe under oblique video microscopy. Force measurement: E,F) A dissected tentacle is laid on a clean glass slide and surrounded by a droplet of seawater. The experimental probe of a tensiometer is lowered through the water onto the tentacle and allowed to adhere to its surface. As the probe descends through the droplet, it is opposed by a buoyant force proportional to the volume of probe that has been submerged (cf. negative slope of the force trace before the magenta circle). At the point of contact with the tentacle (magenta circle), this gradual decrease in force stops and is replaced by a sudden, sharp drop to approximately no force as the probe lifts off from the tensiometer's cantilever sensor as the probe can no longer move down. Then, the probe is retracted from the tentacle until it detaches from the tentacle surface. The difference between the force on the probe as it makes context with the tentacle and the maximum force it experiences before detachment is the "adhesive force" we report (red bar with whiskers). It should be noted however, that this value is in fact a pressure, a force experienced over the contact area of the probe with the tentacle.

$m = 0.000529642$ and intercept of $B = 5.474705$ calculated (Theil's incomplete method, n=22). Thus only a very small proportion of colloblasts (CAF = 1.04%) are activated in response to compression under these conditions.

Effect of probe surface chemistry on adhesive response

A hydrophilic coating of lysine was applied to PLA probes in the investigation of surface chemistry impact on adhesive release. When performed using Dragonskin as a ridge substrate, adhesion events were again visualized in similar numbers to those found using an untreated PLA probe (Fig. 3A). A Spearman ranking test revealed no significant correlation between probed area and the number of adhesion events (Spearman r, P=0.1966, two-tailed). Only 9 area sizes were able to be tested in this study, and thus further studies will be necessary to elucidate any impact of hydrophobic surfaces on adhesion events.

Probing of tentacles using a copepod carcass resulted in an equation closer to that of the untreated PLA probes, with $m = 0.00025$ and $B = -4.35411$ (Theil's incomplete method, n=6) (Fig. 3B), meaning a CAF of 0.491%, just under half of the proportion activated in response to probing. The data also showed a significant positive correlation between contact area and colloblast adhesion events (Spearman r, P=0.0028, two-tailed).

During probe retraction from tentacles, it was possible to visualize the point at which deadhesion events occurred, these distances were collated for all untreated probe contact events (Fig. 4C), for which the median deadhesion event distance was 83.33 μm. This was significantly greater than the median deadhesion event distance for lysine-coated probes (16.48 μm, Dunn's Multiple Comparison test, P<0.0001) or copepod probes (10.73 μm, Dunn's Multiple Comparison test, P<0.0001). However, the distance of deadhesion events was not found to be significantly different between lysine-coated probes and copepod carcass probing (Mann Whitney, P=0.7972).

Compressive force and observed deadhesion modalities

The proportion of deadhesion and colloblast tail severing adhesive termination events were compared between the probing types using Dragonskin as a ridge substrate, and this proportion was not found to be significantly different (Kruskal-Wallis test, P=0.1136, n_{PLA}=23, n_{lysine}=8, $n_{copepod}$=6), indicating the mode of adhesive termination is not affected by probing surface chemistry (Fig. 4A). However, the proportion of deadhesion events was found to differ significantly between untreated PLA probing with an Ecoflex ridge vs a Dragonskin ridge (two-tailed MW test, P=0.0021), with Ecoflex resulting in a significantly lower proportion of deadhesion events compared to Dragonskin (Fig. 4B). Thus, compressive force may play a role in the type of adhesive termination observed, and the proportion of deadhesion events may be inversely related to compressive force.

Baseline force and adhesive buildup/depletion assays

We conducted two series of repeated measurements of the adhesive force arising from a single spot on two different *P. bachei* tentacles (Fig. 5). In one series, we cleaned the measuring probe between measurements, removing any adhesive substances released by the colloblasts. In the other series, the probe was not cleaned, allowing any adhesive substances released by the colloblasts to build up on the probe's surface. Both series began with a starting value of about 200 micronewtons (μN) of adhesive force, which we subsequently take as a rough "baseline" adhesive force value. In the series of trials with probe cleaning, the adhesive force drops asymptotically to zero (fit to the model: $y = 386.8 \cdot e^{-0.6781x}$ with $R^2 = 0.99$). In the series of trials without probe cleaning, the measured adhesive force hovered around the baseline value of 200 μN for the first three trials, after which it gradually increased before plateauing around 300 μN.

The effect of curing time on adhesive force

Though cydippid ctenophores ambush and ensnare their prey, and adhesion is thus presumed to happen rapidly, it is unclear precisely how rapidly adhesion may occur or if the bond may increase in strength if allowed to cure for longer amounts of time. To investigate this, we assayed the effect of curing time on colloblast adhesion by probing the tentacle, this time at a fresh spot on a new tentacle between trials, while varying the length of time the probe was allowed to sit and "cure" on the tentacle surface for either 5, 60, 180, 300, or 600 seconds (Fig. 6). The lowest curing time value of 5 seconds was limited by the response time of the testing apparatus. We observed no statistically significant difference in bond strengths between different curing times (Fig 6.), as assessed by Kruskal-Wallis testing (P-value cutoff of 0.05).

During adhesion visualization experiments, several instances of adhesion were observed following compression for a much shorter duration than 5 seconds. In some instances, adhesion occurred instantaneously with compression, visualized as colloblast adhesion events as the tentacle contracted prior to probe retraction.

Impact of ambient pH on colloblast adhesive force

Ambient pH can significantly affect aquatic life in general and chemical adhesion more specifically, an effect that has been studied extensively in the adhesive system of mussel holdfasts (Carrington et al., 2015; Martinez Rodriguez et al., 2015; O'Donnell et al., 2013). With this in mind, we measured the adhesive force of P. bachei tentacles in artificial seawater adjusted to four different pH conditions: 9.0, 8.2 (approximately "standard" ocean surface pH), 7.0, and 6.0 (Fig. 7). Kruskal-Wallis testing showed a significant difference between the different test conditions (P=0.04) and subsequent pairwise Dunn's testing with Bonferroni correction showed that the only statistically significant difference between the medians was that between pH conditions 7.0 and 8.2 (P=0.0138). We also calculated the moment coefficient of skewness for each condition,

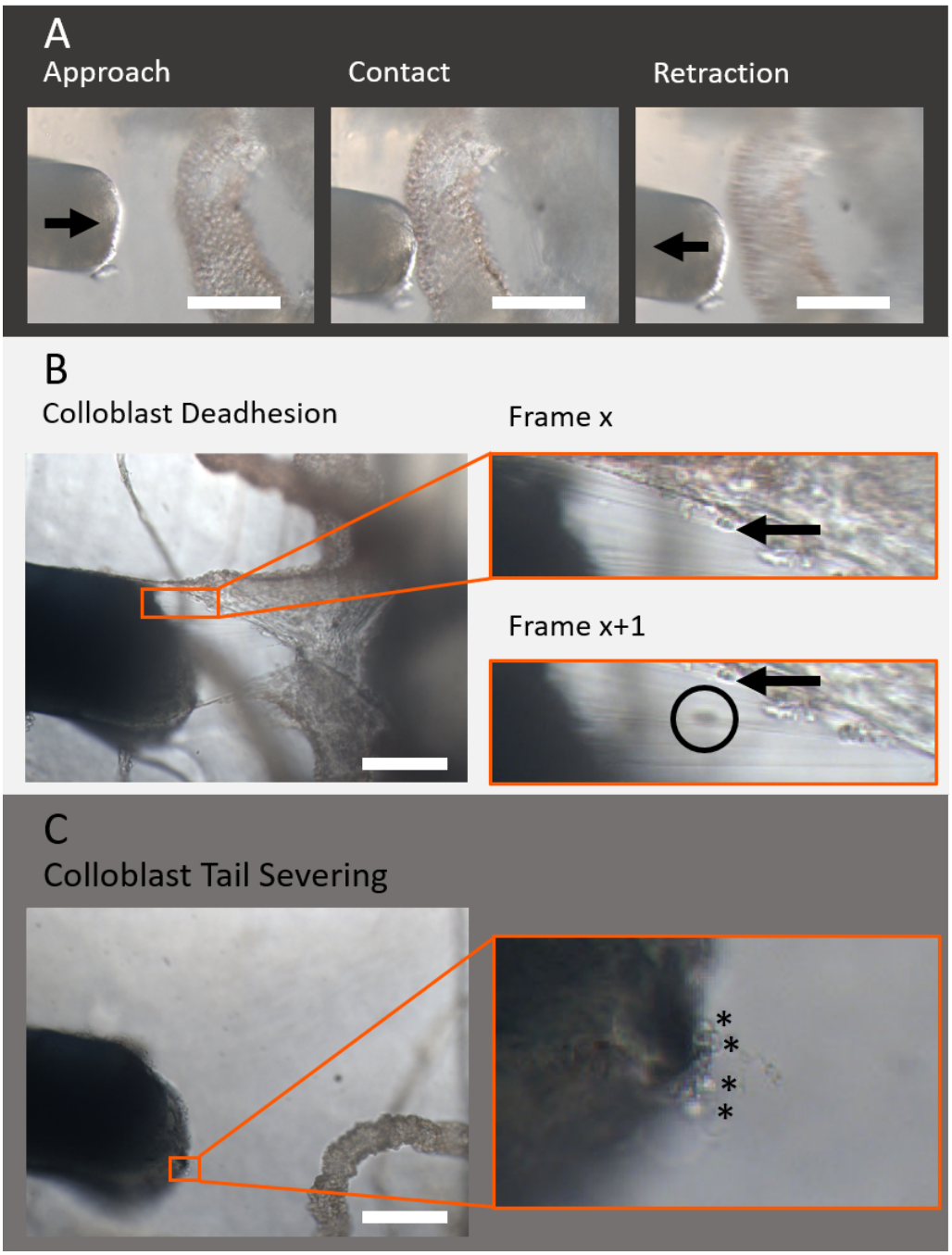

Figure 2. Compression of Tentacles was Required for Adhesion Events and Adhesive Termination to be Visualised. A) Representative images of probe contact without tentacular compression. The probe is brought towards the tentacle until contact is just made. The probe is left stationary for 5 seconds, then retracted. No probing experiments of this type resulted in visualization of adhesion events. B) Representative images highlighting visualization of deadhesion events. As the probe is retracted zooming in to the space between the probe tip and the tentacle core reveals colloblast tails tethering adhered heads on the probe tip to the tentacle core. Further retraction allows for visualization of a colloblast head (black circle) springing back towards the tentacle, having deadhered from the probe tip. Arrow is used to denote landmark feature within both frames. C) Representative images highlighting visualization of colloblast tail severing events by identification of colloblast heads on the probe tip surface following full retraction from the tentacle. The probe is retracted and zoom applied to the probe tip. Colloblast heads appear as spherical objects (*) adhered directly to the probe tip with no colloblast tail tethering it to the tentacle. All scale bars represent 100 μm.

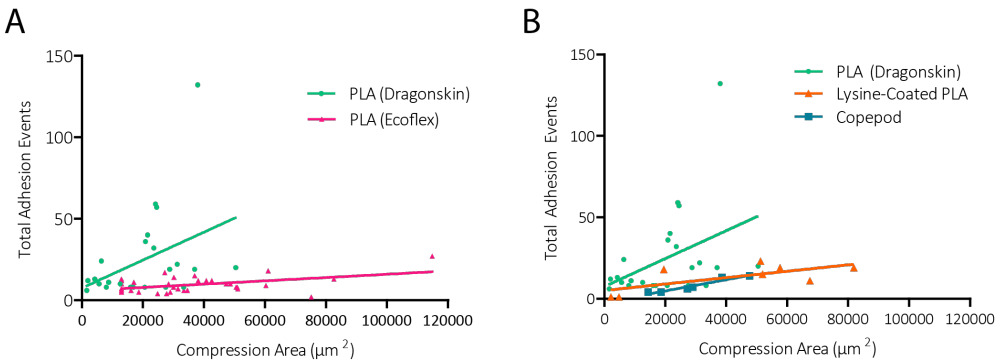

Figure 3. Number of Colloblast Adhesion Events was Dependent on Force Transferred to the Tentacle and on Area of Contact Between Probe and Tentacle. A) Total observed adhesion events for probing trials between severed tentacles and probes of untreated PLA. Two ridge substrates were used, a more flexible Ecoflex, and a more rigid Dragonskin, to assess the impact of compressive force on adhesive events. Spearman r testing revealed a significant positive correlation between compression area and total adhesion events when probing using untreated PLA probes with Dragonskin as a ridge (Spearman r, P=0.0467, $y = 0.000529642x + 5.74706$) but not when using Ecoflex (Spearman r, P=0.1473, $y = 0.0000287345x + 6.88$). B) Total observed adhesion events for probing trials using a Dragonskin ridge with probes of different surface chemistries: untreated PLA, lysine-coated PLA, and copepod carcass. Total adhesion events were plotted against the area of compression induced by the probe. Significant positive correlation was identified in untreated PLA (see (A), PLA: $y = 0.000529642x + 5.74706$) and copepod carcass (Spearman r, P=0.0028, $y = 0.00025x - 4.35411$), but not in lysine-coated probes (Spearman r, P=0.1966, $y = 0.00013x + 23.88775$). All calculated lines of best fit were acquired using Theil's incomplete method for non-parametric data. Note that graphs presented contain the lines of best fit calculated automatically within Prism, not taking into account a non-normally distributed data set.

and found that the data for pH conditions 9, 7, and 6 all have positive skew coefficients (0.40, 0.56, and 0.81 respectively), with mean values exceeding the median values in each of these conditions. This is due to prominent tailing of the data toward higher values of adhesive force, visible in the kernel density estimates around these data in Fig. 7.

Discussion

A subset of colloblasts release adhesive when stimulated

The visualization of adhesion in parallel with the force measurement studies presented here support three commonly presumed properties of colloblast adhesion—that the adhesive is an expendable chemical substance released from the colloblast apical surface, that this adhesive is fast-acting, and that this adhesive can be released in response to physical stimulation (Franc, 19778; Tamm, 2014; von Byern et al., 2010). Visualization of tentacle probing displayed that adhesive is released from only a small number of colloblasts in response to physical stimulation. In our force measurement studies, when a single spot is probed multiple times and the probe is cleaned between trials, the adhesive force precipitously decreases, but if the probe is not cleaned between such trials, the adhesive force gradually increases and plateaus. These observations are consistent with a system in which colloblast activation and adhesive release are discrete events performed by a subset of colloblasts in response to physical stimulation. On each trial in serial force measurements at a single point on the tentacle's surface, the test probe activates some fraction of the colloblasts within that area, causing some colloblasts to release their adhesive onto the probe. In subsequent trials, fewer and fewer colloblasts would be expected to remain intact with their adhesive unreleased. When the probe is cleaned between trials, this appears as a depletion of adhesive force in that spot, and when the probe is not cleaned between trials, this appears as adhesive building up on the probe, gradually reaching a maximum (~300 μN). The maximum expected number of colloblasts in the area probed would be 9,000 (based on maximum contact area of 193,349 μm^2 and a maximum density of colloblasts each with area 21.81 μm^2 orientated in the maximum possible hexagonal packing arrangement), and based on our maximum estimate of colloblast activation we would expect only ~100 to be activated and release adhesive (based on PLA on Dragonskin, for which we have the highest number of experimental replicates). Thus, the force measurement maximum would be expected to be 2 orders of magnitude higher than that recorded if accumulation of the total adhesive was occurring. Therefore, an additional factor must be at play here. While it was not possible to visualize repeat probing of a single area, we have visualised adhesive and colloblast heads deposited on the surface of a probe tip following retraction of a probe, potentially preventing adhesive from re-adhering to the tentacle on re-probing. While this may account for an undervaluation of the maximum force measurement following exhaustive re-probing of an area, it does not account fully for this discrepancy. Perhaps adhesive curing occurs faster than re-probing can occur, and thus the originally deposited adhesive is no longer sticky by the second round of probing. An alternative reason could be that repeat probing of tentacles does not trigger all colloblasts to eventually be triggered. This could represent desensitization of the colloblast adhesive release system to repetitive physical stimulation. Recent evidence postulating colloblasts as neuronal in origin (Babonis et al., 2018) may add weight to this desensitization conjecture, however comprehensive electrophysiological studies on colloblasts during physical stimulation would be necessary to test this.

The fact that adhesive contact between tentacles and probes were visualizable is proof that physical stimulation is a mechanism of stimulating adhesive release, however the lack of adhesion observed with a light tapping of tentacles indicates some threshold of physical force required for adhesive

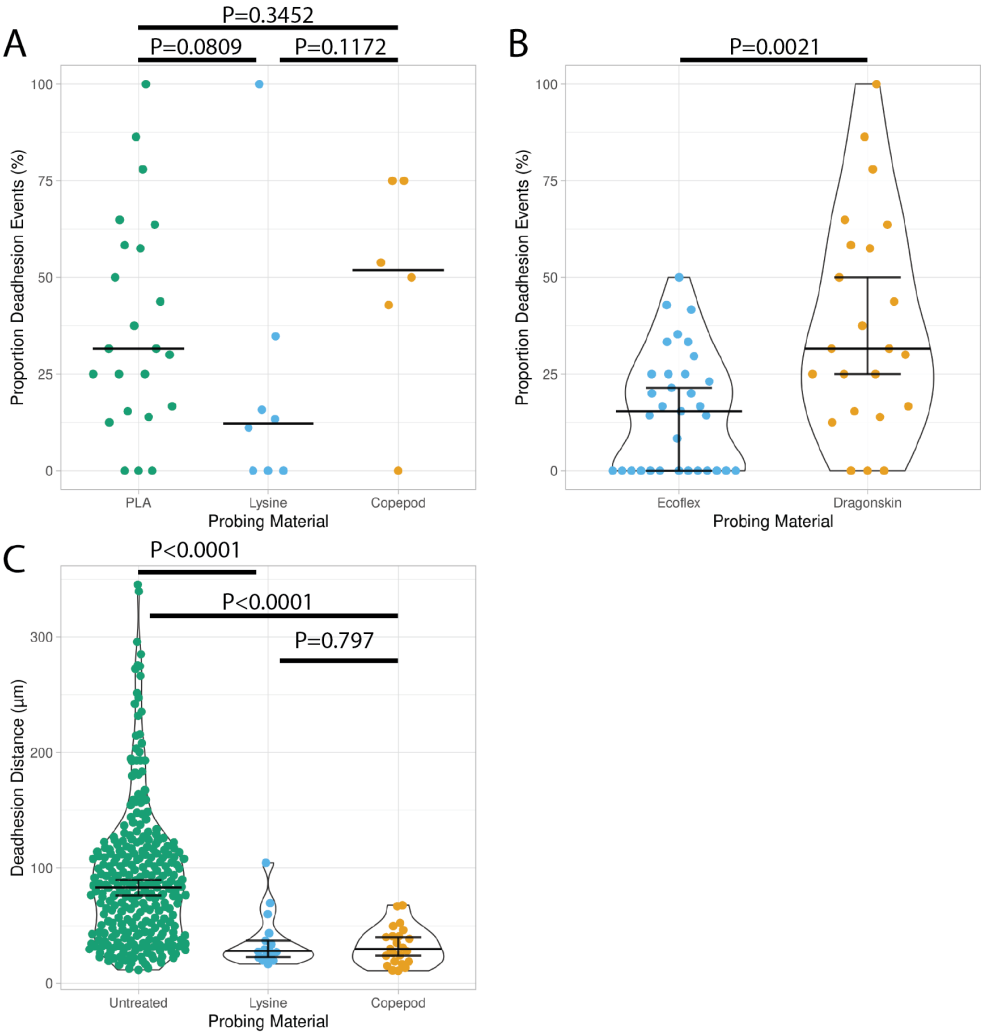

Figure 4. Surface Chemistry of the Probing Surface was Not Found to Significantly Effect on Adhesion Termination Modality Proportion but Did Impact Distance of Deadhesion. Proportion of observed adhesion termination events classified as deadhesion events (colloblast head detaching from the probe tip) in each probing trial for each probe type used, all measurements taken using Dragonskin as a ridge substrate. Statistics performed using Kruskal-Wallace and Mann Whitney tests. Median shown as solid black bar. B) Proportion of observed adhesion termination events classified as deadhesion events using untreated PLA probes with either an Ecoflex or a Dragonskin ridge. Bars show mean +/-95% CI. Statistics performed using Mann Whitney test. C) Linear distance (μm) between tentacle surface and adhered colloblast head in the frame prior to head deadhesion event, compared between probing using untreated PLA probes, lysine-coated PLA probes, and copepod carcasses, data for all probing trials collated together, statistical analyses performed using Kruskal-Wallace and Mann Whitney tests.

release. The slope of the line is an order of magnitude larger when compressing against Dragonskin than Ecoflex, the only difference in experimental conditions being that Dragonskin is substantially firmer than Ecoflex, which represents a more deformable silicone (shore-hardness scores of 10A and 00-10, respectively). The reduced deformation in Dragonskin may be allowing a greater force to be passed from the probe to the tentacle surface, as opposed to being absorbed via Ecoflex deformation, and thus implies a force or pressure sensitive mechanism in colloblast adhesive release. The proportion of the two adhesion termination modalities was different when probing against a firm substrate vs a more flexible substrate, indicating that bonding strength between the colloblasts and the probe may depend on the initial force exerted on the tentacle. It would be assumed that higher force exerted on the colloblasts would induce them to release adhesive more fully, which would result in a higher bonding strength between the colloblast head and the probe, compared to the tensile strength of the extended colloblast tail. Counterintuitively, the reverse is observed in the visualization studies, and more studies are required to determine the cause of this difference.

Colloblast adhesive cures rapidly under variable environmental conditions

The adhesive in ctenophore colloblasts also acts rapidly: the adhesive force measured when the probe had been allowed to cure for 5 seconds was comparable to the force measured when it had been allowed to cure for 10 minutes. The adhesive is likely fully cured in less than 5 seconds' time, as shown in incidental recordings of low contact-time probing during the visualization studies. Given that tentaculate ctenophores are ambush/entanglement-predators not unlike spiders in their approach to feeding, this is a reasonable

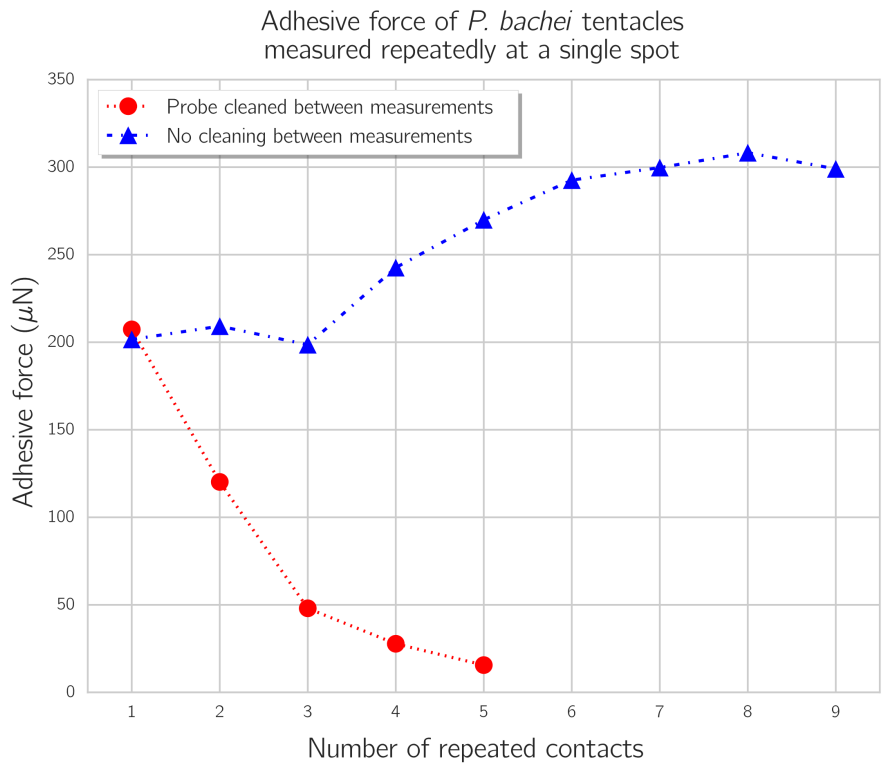

Figure 5: Plot of adhesive forces from repeated measurements at a single spot on two different *P. bachei* tentacles with two different testing protocols. Between trials, the testing probe was either cleaned, presumably removing any residual adhesive, or left uncleaned, presumably allowing adhesive to build up on the surface of the probe until all available adhesive at that spot is depleted.

conjecture.

Interestingly, colloblast adhesive appears to function with similar efficiency across the wide range of ambient pH values tested. This implies that either the adhesive substance and its chemical mechanism of adhesion are relatively resistant to shifts in pH or that the pH of the adhesive granules themselves is controlled or buffered and adhesion occurs rapidly after the granules rupture, leaving little time between granule rupture and bonding to prey for pH to effect adhesion.

Colloblast adhesive is relatively strong, but the colloblast adhesive system is relatively weak

For our force-measurement tests, we utilized a tensiometer probe with hydrophilic surface chemistry. This type of surface is useful because it strongly maintains a layer of water around the probe that must be displaced or coordinated with for colloblast adhesive to adhere to the probe's surface. Ctenophore prey items in the wild likely run a wide gamut of surface chemistries that are difficult to characterize in practice, but our approach provides a reasonable baseline by making water a significant barrier to interacting with the probe surface. Adhesion visualization revealed that non-biological probes resulted in a similar effect as using a deceased prey carcass, further validating this assumption.

If we compare the adhesive strength of *Pleurobrachia* colloblasts to other studied biological adhesive systems in terms of force per unit area, colloblast adhesive appears relatively weak (Fig. 8). Based on Eq. 3 the expected number of colloblasts initially adhering to the force measurement probe is ~100 colloblasts (based on $m = 0.000529642$ $colloblasts \cdot \mu m^2$, $A_{contact} = 193,349 \mu m^2$, and $B = 5.47$). From our 200 μN baseline force measurement, this yields an estimate of ~2 μN of adhesive strength per active colloblast. If all 9,000 colloblasts beneath the surface area of the same probe activated at once, this would result in ~18,000 μN of adhesion across ~0.2 mm^2, or 90,000 $N \cdot m^{-2}$, a rough estimate of the strength of the adhesive considered on its own. The baseline force estimate of ~200 μN of adhesive force across that same ~0.2 mm^2 area (1,000 $N \cdot m^{-2}$) represents the effective strength of the colloblast adhesive system under working conditions.

This means that the strength of colloblast adhesive itself is on par with that of systems involved in anchoring whole animals such as mussel holdfasts (Fig. 8), and gecko foot setae (Autumn et al., 2000; Lin et al., 2007; Waite, 2017). This is particularly notable given that mussel holdfast adhesives may be biochemically similar to Pleurobrachia colloblast adhesive (Townsend and Sweeney, 2019). However, the adhesive strength of the colloblast system as a whole is much weaker than these whole-animal anchoring systems, and under working conditions colloblasts adhere to prey with a force on the same order of magnitude as orb weaver spider webs' viscous capture threads (Opell and Hendricks, 2007).

Modelling of ctenophore prey capture with a weak adhesive system suggests a mechanism for prey selection

It's clear from both field and laboratory observations that ctenophore colloblasts are sufficiently sticky to capture

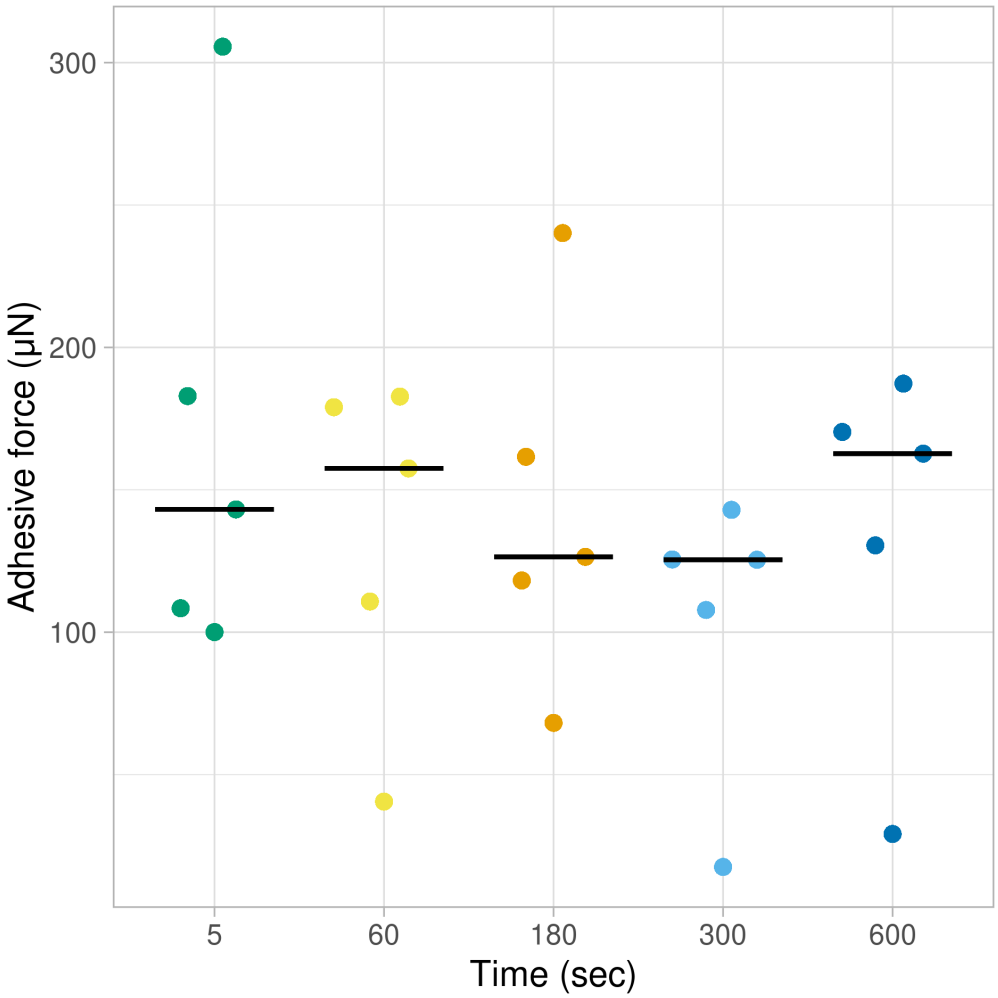

Figure 6: Adhesive force did not significantly depend on the amount of time that the adhesive was allowed to cure. No curing time trial groups' medians differ by Kruskal-Wallis rank sum test, suggesting that *P. bachei* colloblast adhesive both acts rapidly and once attached, may remain bonded for some time. Filled circles = data points; black lines = median values.

the prey they regularly encounter (Bishop, 1968; Franc, 1978; Greene et al., 1986). However, it's not immediately obvious why *Pleurobrachia* might employ such a strategy: using a strong adhesive sparingly to produce an overall weakly-adhering system. While an evolutionary answer to this question is a matter outside the scope of this study, our data allow us to suggest one potential explanation of how the unique properties of the ctenophore adhesive system might be particularly useful. Here, we present a model describing how a relatively weak adhesive system can mechanically filter prey by size for an animal otherwise lacking the ability to "see" their quarry.

Pleurobrachia commonly prey upon small animals such as copepods (Haddock, 2007; Tamm, 2014). They utilize an ambush hunting strategy reminiscent of orb-weaver spiders (Greene et al., 1986)—extending their tentacles and fanning out their numerous secondary tentilla, waiting for prey to close in, and ensnaring them in this sticky "web." The close arrangement of tentilla increases the likelihood that prey items encountering the net will interact with, and become entangled in, multiple tentilla. This entanglement phenomenon, and the fact that the tentacular apparatus is a living organ whose loss or damage has a negative impact on feeding, are each essential to understanding how ctenophores may leverage their low-strength adhesive system to discern and handle appropriately sized prey.

Consider a hypothetical prey item, modeled as a sphere with a radius, r_{prey} that has values within a range of 0.1–3.0 mm, which encompasses the range of nauplii and copepod sizes (radii of approximately 0.11–1.5 mm) for which data on *Pleurobrachia* prey capture exist in addition to hypothetical prey larger than those known to be reliably captured by *Pleurobrachia*. This prey has a mass, m_{prey} based on a copepod density value, ρ_{prey}, of 1,050 $kg \cdot m^{-3}$ as estimated from available literature (Knutsen et al., 2001), thus,

Eq. 4 $m_{prey}(r_{prey}) = \frac{4}{3}\pi r_{prey}^3 \cdot \rho_{prey}$

When an individual tentillum, measured from our micrographs to be 30 microns wide ($w_{tentacle}$), makes contact with the prey, it wraps a third of the way around the sphere's circumference and adheres with a contact area, $A_{contact}$

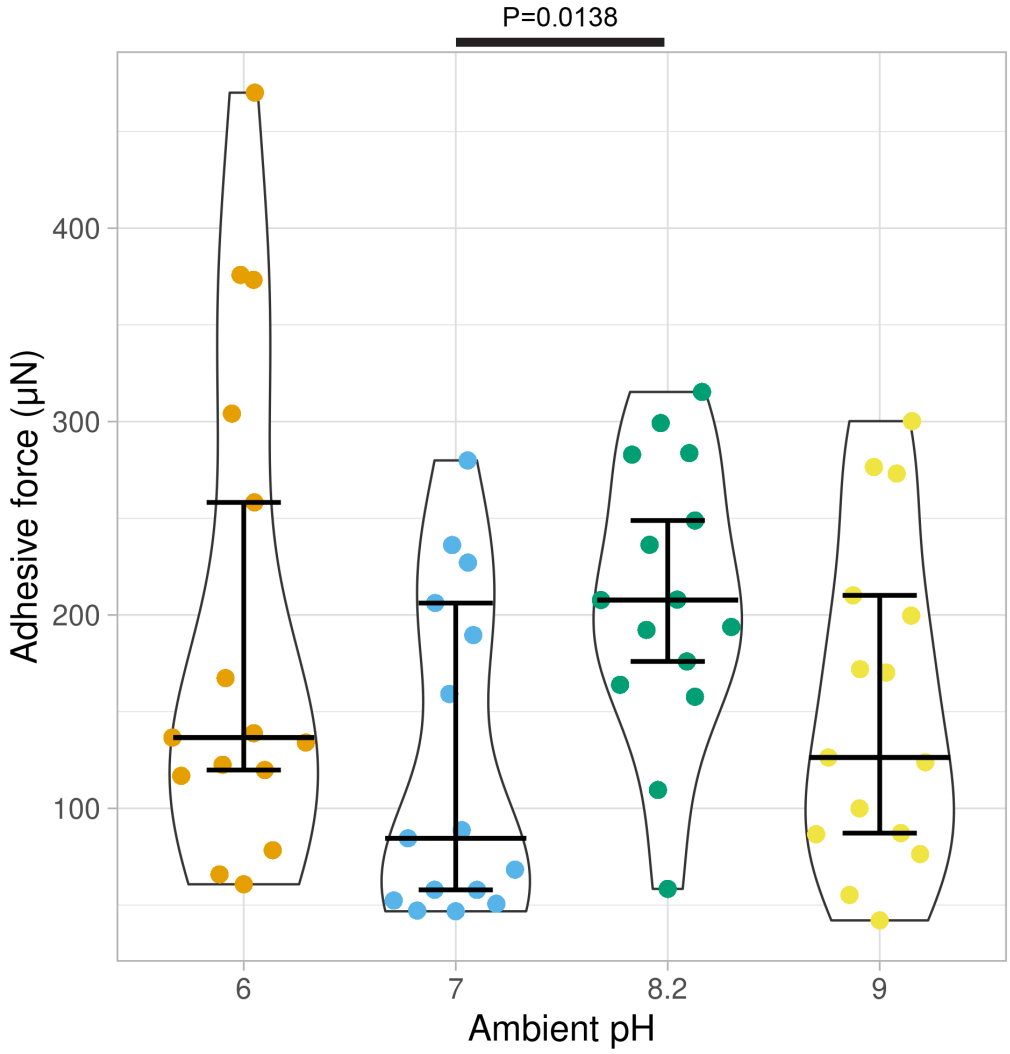

Figure 7: Under varying ambient pH conditions P. bachei tentacles show similar median adhesive forces. Kruskal-Wallis testing followed by pairwise Dunn's tests showed that adhesive strength differed significantly only between the ambient pH 7 and 8.2 trial groups. The distribution of observed adhesive forces in all trial groups besides pH 8.2 showed substantial positive skew, visible in the kernel density estimates of the above violin plots. Black bars = 95% confidence interval about the median.

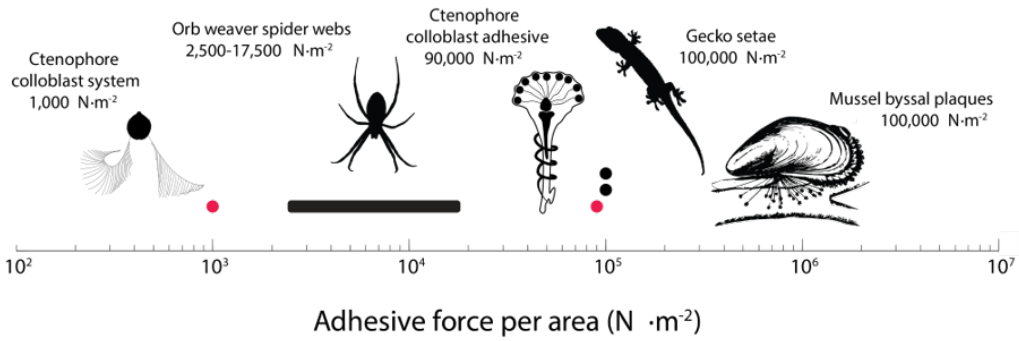

Figure 8: Comparison of various biological adhesive systems by adhesive force per unit area. The adhesive force generated by the colloblast adhesive system is among the lowest of biological systems that have been examined, though the adhesive itself is relatively strong. Ctenophore, orb weaver spider, and gecko silhouettes downloaded from the PhyloPic database (http://phylopic.org). Mussel silhouette created from a public domain image from the Freshwater and Marine Image Bank at the University of Washington. Pink circles, force values observed in *Pleurobrachia*; black circles, forces observed in non-ctenophore adhesive systems.

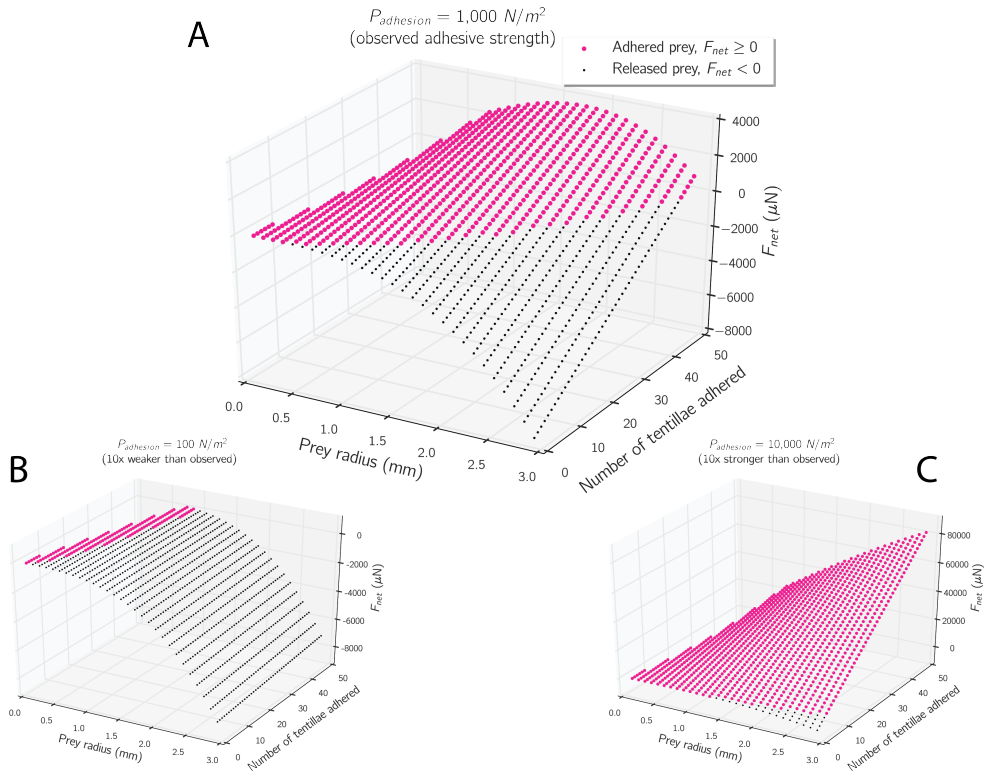

Figure 9: Modelling the net force on hypothetical escaping prey items adhered to multiple ctenophore tentilla. If F_{net} is positive, the adhesive force exceeds the opposing escape force, and the prey remains stuck (pink circles). If F_{net} is negative, the escape force wins out, and the prey is released from the tentilla (black circles). Only an adhesive of the approximate order of magnitude strength as we observed (A) allows for a relatively wide range of acceptable prey while still allowing for the release of very large prey (1.5 mm radius). If the adhesive's strength were 10 times weaker (B), only a very narrow range of very small prey could be captured, whereas if it were 10 times stronger (C), prey items of unmanageably large sizes not reliably handled in nature would easily adhere to even a single tentillum, potentially exposing the animal to injury.

Eq. 5 $A_{contact}(r_{prey}) = \frac{2\pi r_{prey}}{3} \cdot w_{tentacle}$

In this model, additional tentilla can contact the prey and potentially adhere in the same fashion. Our visualization studies were performed on single linear segments of tentacle,and thus it is unclear whether contact with additional tentilla would result in a different response. Similarly, it is possible that in a natural setting, more colloblasts could be activated in response to environmental cues to subdue struggling prey on an area of existing contact and adhesion, increasing adhesive strength without more tentilla making contact, but more studies of the underlying control mechanisms of adhesive release will be needed to assess this. The total adhesive force is proportional to the surface area of all tentilla adhered to the prey, given the measured adhesive strength value, $P_{adhesion}$, of ~1000 $N \cdot m^{-2}$ (computed from the observed value of ~200 μN over a flat, circular probe with a 0.5 mm diameter, and knowing a proportional increase of 0.000529642 colloblasts per μm^2, each adhering with a force of 2 μN). As an escape response, prey accelerate directly away from the adhering surface of the tentacle, generating a maximum force proportional to their mass, as inferred from video analyses and hydrodynamic modeling of copepod escape behavior (Kiørboe et al., 2010). For this model, we consider a representative value for the mass-specific force of 100 $N \cdot kg^{-1}$. The units of mass-specific force ($N \cdot kg^{-1}$) are equivalent to those of acceleration ($m \cdot s^{-2}$) so we denote the value in our model as a_{prey}. From these premises, we can construct the following model for total adhesive force and escape force,

Eq. 6 $F_{adhesion}(n, r_{prey}) = n \cdot A_{contact}(r_{prey}) \cdot P_{adhesion}$

Eq. 7 $F_{escape}(r_{prey}) = m_{prey}(r_{prey}) \cdot a_{prey}$

Because we take these forces to be directly opposed to one another, we can compute and plot the difference of these forces,

Eq. 8 $F_{net}(n, r_{prey}) = F_{adhesion}(n, r_{prey}) - F_{escape}(r_{prey})$

Thus, when F_{net} is positive, the force of adhesion is greater than the force of the prey attempting to escape, and the prey remains adhered. When F_{net} is negative, the escape force wins out, and the animal is released. We consider n within a range of 1 (a single tentillum) to 50 (approximately the total number of tentilla present on an entire single adult Pleurobrachia tentacle, estimated from photographs). We compute F_{net} only when the condition $n.w_{tentacle} \leq 2r_{prey}$ is satisfied, a rough boundary condition reflecting that a prey item cannot have more than its diameter's worth of tentacles adhered across its surface.

Plotting $F_{net}(n, r_{prey})$ using the observed value for

$P_{adhesion}$ in *Pleurobrachia* tentacles of 1,000 $N \cdot m^{-2}$ (Fig. 9A), reveals several interesting patterns. Small prey items with radii less than 0.5 mm adhere and stay adhered on contact with even a single tentillum. Making contact with other tentilla only enhances this effect. A medium-sized prey item with a radius of 0.5-0.7 mm however, must make contact with two to three tentilla in order to stay adhered, while large prey models, such as the model with a radius of 1.5 mm, escape unless 12 or more tentilla adhere to it. The largest prey models shown, between 2.5 and 3.0 mm, will not stay adhered unless they make contact with two thirds or more of the tentilla on the entire tentacle. Because $F_{adhesion}$ is dependent on the available contact area, and thus the prey radius, the slope of F_{net} as a function of tentacles adhered increases with increasing prey size.

The overall pattern of size-dependent prey capture rates depicted in this model is consistent with laboratory observations of *Pleurobrachia* feeding (Greene et al., 1986). Although the distance between tentilla can vary based on how relaxed the tentacles are overall, and the tentilla are allowed to drift freely in 3D, an approximate 0.5-1.0 mm spacing between tentilla is a reasonable estimate for most conditions. Intuitively then, one would not expect even a prey item 3 mm in total length to make contact with the 12 tentilla needed for its capture, even under ideal circumstances, whereas prey 1 mm in total length likely stand a better chance of making contact with the two tentilla necessary for successful adhesive capture.

Real-world prey introduce a number of other factors including irregular surface geometry and the effects of entanglement on the ability to produce an effective escape response, but this model illustrates a key point for understanding why colloblast adhesive may be so weak compared to other systems. Namely, ctenophores appear to rely on multiple tentilla adhering to prey to both provide sufficient adhesive force and spread out the potentially damaging force that attempted prey escape responses generate.

This overall effect is critical for ctenophores. Lacking any familiar means to sense the size of the prey that they are encountering as they lay in ambush, ctenophores need some means to accept prey of a size that they can restrain and consume and reject those items that it cannot. There is evidence that cydippid ctenophores like *P. bachei* are capable of autotomizing their tentilla under duress (Glynn et al., 2014; Moss et al., 2004), but subsequent regeneration of tentacular tissue introduces a significant metabolic cost (Bading et al., 2017; Maginnis, 2006). The prey capture system described by our model may help to mitigate these risks. Here, prey are mechanically sorted by size via a low strength adhesive system requiring multiple points of contact in order to capture larger prey. This minimizes the risk that a ctenophore will overinvest in prey that are too large for them to handle or consume without injury. Additionally, the relatively low proportion of colloblasts activated in any prey-contact scenario further reduces the risk of losing excessive numbers of colloblasts in the event of a failed feeding event, meaning the tentacle would be capable of re-adhering to new prey in a potentially short timeframe. If we consider the same model as described above, modifying only the value of $P_{adhesion}$ to be 10 times weaker at 100 $N \cdot m^{-2}$, we obtain a model ctenophore that needs many tentilla to adhere to catch even the smallest prey items (Fig. 9B). This hypothetical animal is safe from biting off more than it can chew, but is unlikely to capture all but the smallest prey. If the adhesive strength parameter is made 10 times larger than the observed value, such that $P_{adhesion} = 10,000$ $N \cdot m^{-2}$, we see that most model prey items considered strongly adhere with only one or two tentilla attached (Fig. 9C). Even prey with diameters of 6 mm, a size approaching the centimeter length scale corresponding to the total body length of an adult Pleurobrachia, are within reach for this hypothetical ctenophore, requiring only 5 tentilla to adhere before they can be restrained. These large prey items present increasing risk for injury, with a decreasing likelihood of successful handling and feeding. In laboratory conditions, successful capture and handling of prey items in excess of 1.5 mm of total length is very rare (Greene et al., 1986). Large prey such as these tend to detach and escape rather than causing damage, but a very strong adhesive system, as with a stronger adhesive or with a higher proportion of colloblasts activated, might preclude this safe rejection and release mechanism. The measured adhesive system strength of 1,000 $N \cdot m^{-2}$ allows Pleurobrachia to occupy a happy biomechanical medium, where a range of reasonable prey sizes can be reliably handled, while larger, potentially stronger prey are allowed to safely detach.

The biomechanical analogy between ctenophore tentacles and orb-weaver spider webs may run deeper still if there is any correspondence between mean tentilla spacing and average prey size between different species of ctenophores, or if ctenophores of a single species can modulate tentilla spacing as a function of behavior or development to select for different prey. This would be similar to the effect of mesh spacing in spider webs on retained prey, a different kind of biomechanical prey filtering mechanism observed under a variety of experimental conditions (Blackledge and Zevenbergen, 2006; Chacón and Eberhard, 1980; Harmer et al., 2015; Herberstein and Heiling, 2013). Further observations of diverse ctenophore feeding behavior, both *in situ* and in the lab will be necessary to address this point.

Concluding Remarks

We measured the adhesive strength of the colloblast adhesive system in the ctenophore *P. bachei* by adapting an instrument for measuring surface tension and a probe of known surface chemistry and geometry to determine the force required to detach this probe once it had bonded to live, dissected tentacles. Using this setup, we demonstrated that colloblast adhesive is released destructively and bonds to its target in seconds, confirming two key properties of these one-time-use cells. Visualization of probing events using the closely related species, *P. pileus* confirmed this destructive process through visualization of colloblast detachment from tentacles

and allowed for calculation of colloblast adhesive strength. Furthermore, we showed that the bonding of this adhesive was robust to a wide range of ambient pH conditions. Surprisingly, while we found that individual colloblasts are not weak, the adhesive system as a whole is among the weakest yet studied, because the majority of colloblasts do not activate on contact. By considering colloblast adhesive in the context of *Pleurobrachia* feeding behavior and modeling a range of prey size and tentilla contact scenarios, we postulate that this low-strength adhesive system may serve a key purpose. *Pleurobrachia* rely on prey colliding with the animal's meshwork of tentilla, which are themselves an organ whose damage would put the animal at a disadvantage in feeding. With no way to otherwise "see" directly what prey they are catching or how massive it is, ctenophores need a mechanism to select for appropriate prey items. Colloblast adhesive system's relatively low strength means that for all but the smallest prey items, multiple points of contact are necessary to trigger sufficient colloblast adhesive release to securely handle potential prey, and that above a certain size, it is unlikely that enough contact can be made to secure the catch, allowing these very large prey items to safely terminate adhesion without doing substantial damage to the ctenophore. These observations suggest that the control of ctenophore colloblast adhesive release may be tuned to facilitate the complex task of passively selecting appropriate prey.

List of symbols used:

$C_{adhered}$- number of adhered colloblasts
$C_{contact}$ - number of colloblasts contacted by probe
$A_{compression}$ - area compressed by probe (μm^2)
$SA_{colloblast}$ - surface area of an individual colloblast
B - constant applied to linear model equations
n_{PLA} - number of PLA trials
n_{lysine} - number of lysine-coated PLA probing trials
$n_{copepod}$ - number of copepod probing trials
m_{prey} – prey mass
r_{prey} – prey radius
ρ_{prey} – mass density of prey
$A_{contact}$ – contact area of prey with tentilla
$w_{tentacle}$ – tentilla width
n – number of tentilla adhered
$P_{adhesion}$ – adhesive pressure exerted by adhesive material
a_{prey} – mass-specific escape force (escape acceleration)
$F_{adhesion}$ – total adhesive force restraining prey
F_{escape} – total escaping force generated by prey
F_{net} – net force acting on prey

Acknowledgements

Drs. Alison Sweeney, Paul Janmey, Mike LaBarbera, Jack Costello, and Thomas C Collin provided comments that improved the manuscript.

Competing Interests

The authors have no competing interests to report.

Funding

G. P. Castellanos was supported by an REU through NSF grant DMR-1359351. This work was also supported by NSF-1351935 to A.M. Sweeney. G. O. T. Merces was supported by funding from University College Dublin School of Medicine.

References

Alié, A., Leclère, L., Jager, M., Dayraud, C., Chang, P., Le Guyader, H., Quéinnec, E. and Manuel, M. (2011). Somatic stem cells express Piwi and Vasa genes in an adult ctenophore: Ancient association of "germline genes" with stemness. Dev. Biol. 350, 183–197.

Autumn, K., Liang, Y. A., Hsieh, S. T., Zesch, W., Chan, W. P., Kenny, T. W., Fearing, R. and Full, R. J. (2000). Adhesive force of a single gecko foot-hair. Nature 405, 681–685.

Babonis, L. S., DeBiasse, M. B., Francis, W. R., Christianson, L. M., Moss, A. G., Haddock, S. H. D., Martindale, M. Q. and Ryan, J. F. (2018). Integrating Embryonic Development and Evolutionary History to Characterize Tentacle-Specific Cell Types in a Ctenophore. Mol. Biol. Evol. 35, 2940–2956.

Bading, K. T., Kaehlert, S., Chi, X., Jaspers, C., Martindale, M. Q. and Javidpour, J. (2017). Food availability drives plastic self-repair response in a basal metazoan- case study on the ctenophore Mnemiopsis leidyi A. Agassiz 1865. Sci. Rep. 7, 16419.

Bishop, J. W. (1968). A Comparative Study of Feeding Rates of Tentaculate Ctenophores. Ecology 49, 996–997.

Blackledge, T. A. and Zevenbergen, J. M. (2006). Mesh Width Influences Prey Retention in Spider Orb Webs. Ethology 112, 1194–1201.

Carrington, E., Waite, J. H., Sarà, G. and Sebens, K. P. (2015). Mussels as a Model System for Integrative Ecomechanics. Annu. Rev. Mar. Sci. 7, 443–469.

Chacón, P. and Eberhard, W. G. (1980). Factors affecting numbers and kinds of prey caught in artificial spider webs, with consideration of how orb-web trap prey. Bull. Br. Arachnol. Soc. 5, 29–38.

Courtney, A., Alvey, L. M., Merces, G. O. T., Burke, N. and Pickering, M. (2020). The Flexiscope: a low cost, flexible, convertible and modular microscope with automated scanning and micromanipulation. R. Soc. Open Sci. 7, 191949.

Courtney, A., Merces, G. O. T. and Pickering, M. (2020). Characterising the Behaviour of the Ctenophore Pleurobrachia pileus in a Laboratory Aquaculture System. bioRxiv 2020.05.25.114744.

Dunn, C. W., Leys, S. P. and Haddock, S. H. D. (2015). The hidden biology of sponges and ctenophores. Trends Ecol. Evol. 30, 282–291.

Franc, J.-M. (1978). Organization and Function of Ctenophore Colloblasts: An Ultrastructural Study. Biol. Bull. 155, 527.

Glynn, P. W., Bayer, F. M. and Renegar, D. A. (2014). Coeloplana waltoni, a new species of minute benthic ctenophore (Ctenophora: Platyctenida) from south Florida. Proc. Biol. Soc. Wash. 127, 423–436.

Greene, C. H., Landry, M. R. and Monger, B. C. (1986). Foraging Behavior and Prey Selection by the Ambush Entangling Predator Pleurobrachia Bachei. Ecology 67, 1493–1501.

Haddock, S. H. D. (2007). Comparative feeding behavior of planktonic ctenophores. Integr. Comp. Biol. 47, 847–853.

Harmer, A. M. T., Clausen, P. D., Wroe, S. and Madin, J. S. (2015). Large orb-webs adapted to maximise total biomass not rare, large prey. Sci. Rep. 5, 14121.

Herberstein, M. E. and Heiling, A. M. (2013). Does mesh height influence prey length in orb-web spiders (Araneae)? EJE 95, 367–371.

Hernandez-Nicaise, M.-L. (1991). Ctenophora. In Microscopic Anatomy of Invertebrates: Placozoa, Porifera, Cnidaria, and Ctenophora, pp. 359–418. New York, NY: Wiley.

Holstein, T. and Tardent, P. (1984). An ultrahigh-speed analysis of exocytosis: nematocyst discharge. Science 223, 830–833.

Kass-Simon, G. and Scappaticci, Jr., A. A. (2002). The behavioral and developmental physiology of nematocysts. Can. J. Zool. 80, 1772–1794.

Kiørboe, T., Andersen, A., Langlois, V. J. and Jakobsen, H. H. (2010). Unsteady motion: escape jumps in planktonic copepods, their kinematics and energetics. J. R. Soc. Interface 7, 1591–1602.

Knutsen, T., Melle, W. and Calise, L. (2001). Determining the mass density of marine copepods and their eggs with a critical focus on some of the previously used methods. J. Plankton Res. 23, 859–873.

Lin, Q., Gourdon, D., Sun, C., Holten-Andersen, N., Anderson, T. H., Waite, J. H. and Israelachvili, J. N. (2007). Adhesion mechanisms of the mussel foot proteins mfp-1 and mfp-3. Proc. Natl. Acad. Sci. 104, 3782–3786.

Maginnis, T. L. (2006). The costs of autotomy and regeneration in animals: a review and framework for future research. Behav. Ecol. 17, 857–872.

Martinez Rodriguez, N. R., Das, S., Kaufman, Y., Israelachvili, J. N. and Waite, J. H. (2015). Interfacial pH during mussel adhesive plaque formation. Biofouling 31, 221–227.

Moss, A. G., Wells, B. and Muellner, L. (2004). A mechanosensory system that controls feeding in adult Mnemiopsis. In Coelenterate Biology 2003, pp. 145–153. Springer, Dordrecht.

Nüchter, T., Benoit, M., Engel, U., Özbek, S. and Holstein, T. W. (2006). Nanosecond-scale kinetics of nematocyst discharge. Curr. Biol. 16, R316–R318.

O'Donnell, M. J., George, M. N. and Carrington, E. (2013). Mussel byssus attachment weakened by ocean acidification. Nat. Clim. Change. Opell, B. D. and Hendricks, M. L. (2007). Adhesive recruitment by the viscous capture threads of araneoid orb-weaving spiders. J. Exp. Biol. 210, 553–560.

Ryan, J. F., Pang, K., Schnitzler, C. E., Nguyen, A.-D., Moreland, R. T., Simmons, D. K., Koch, B. J., Francis, W. R., Havlak, P., Smith, S. A., et al. (2013). The Genome of the Ctenophore Mnemiopsis leidyi and Its Implications for Cell Type Evolution. Science 342, 1242592.

Schindelin, J., Arganda-Carreras, I., Frise, E., Kaynig, V., Longair, M., Pietzsch, T., Preibisch, S., Rueden, C., Saalfeld, S., Schmid, B., et al. (2012). Fiji: an open-source platform for biological-image analysis. Nat. Methods 9, 676–682.

Townsend, J. P. and Sweeney, A. M. (2019). Catecholic Compounds in Ctenophore Colloblast and Nerve Net Proteins Suggest a Structural Role for DOPA-Like Molecules in an Early-Diverging Animal Lineage. Biol. Bull. 236, 55–65.

von Byern, J., Mills, C. and Flammang, P. (2010). Bonding Tactics in Ctenophores — Morphology and Function of the Colloblast System. In Biological Adhesive Systems, pp. 29–40. Springer-Verlag Wien.

Waite, J. H. (2017). Mussel adhesion – essential footwork. J. Exp. Biol. 220, 517–530.